EF-G Mutations Reveal Correlation between Power Stroke and Translocation Fidelity in Protein Synthesis

Yanjun Chen,[1†] Jacob H. Steele,[2†] Shoujun Xu,[1*] Yuhong Wang[1,2*]

[1]*Department of Chemistry,* [2]*Department of Biology and Biochemistry*

University of Houston, Houston, TX 77204, USA

[†]These authors contributed equally to this work.

*Corresponding authors. Email: sxu7@uh.edu (S.X.), ywang60@uh.edu (Y.W.)

ABSTRACT

The ribosome translocates on the mRNA by primarily three nucleotides per step during protein synthesis, a process catalyzed by elongation factor G (EF-G). The large conformational changes of EF-G in this process generate significant mechanical force, referred to as power stroke. Quantification of power stroke remains under debate and its potential correlation with translocation fidelity has not been observed. In this work, we present a unique application of quantum sensing in combined measurements of the power strokes of mutated EF-G and their influence on ribosome translocation steps. Two EF-G mutants, H584K and Q508K, were expressed, with the mutated residues directly interacting with tRNA. H584K, which interacts on codon-anticodon minihelix, produced a much reduced power stroke of 60 ± 6 pN and induced -1 frameshifting, wherein the ribosome translocated only two nucleotides on both sides of the mRNA. In contrast, Q508K, which interacts with tRNA residue 37 immediately outside the codon-anticodon minihelix, exhibited a power stroke of 89 ± 11 pN and maintained canonical 3-nt translocation, similar to wild-type EF-G. These findings provide direct mechanistic evidence that

the pivotal point and force projection exerted by EF-G are critical for maintaining translocation fidelity, likely via lowering the kinetic energy barrier.

KEY WORDS: ribosome translocation, elongation factor G, power stroke, force spectroscopy, frameshifting, quantum sensing

INTRODUCTION

Protein synthesis by the ribosome is one of the most fundamental biological functions.[1-3] It is critical for the ribosomes to translocate on the messenger RNA (mRNA) by exactly three nucleotides (nts) per step to produce the correct protein sequence.[4, 5] As depicted in Figure 1, mRNA threads through the two subunits of the ribosome, the 50S and 30S subunits in bacteria. The E, P, and A sites are initially aligned, and the transfer RNA (tRNA) is bound at the A site. Elongation factor G (EF-G), in complex with guanosine triphosphate (GTP), accelerates and stabilizes the ribosome's twisting motions while itself undergoes a large conformational change driven by GTP hydrolysis. Subsequently EF-G is released in complex with GDP.[6-8] The mechanism of this complex process involves two key components: the power stroke produced by EF-G and the precise three-nts displacement of the ribosome. An intriguing question is whether these two factors are correlated for maintaining the ribosome on the correct reading frame.[9] To investigate this correlation, the Q508K and H584K mutants (*E. coli* EF-G sequence, numbered from the first methionine) will be utilized to determine how alterations in EF-G's power stroke impact translocation efficiency and fidelity. These mutants were selected because structural and functional studies have shown they are highly conserved sites in domain IV of EF-G, potentially playing

significant roles in maintaining mRNA reading frame. Some variations are shown to be lethal, drastically reducing the translocation kinetics and causing high-percentage frameshifting.[10, 11]

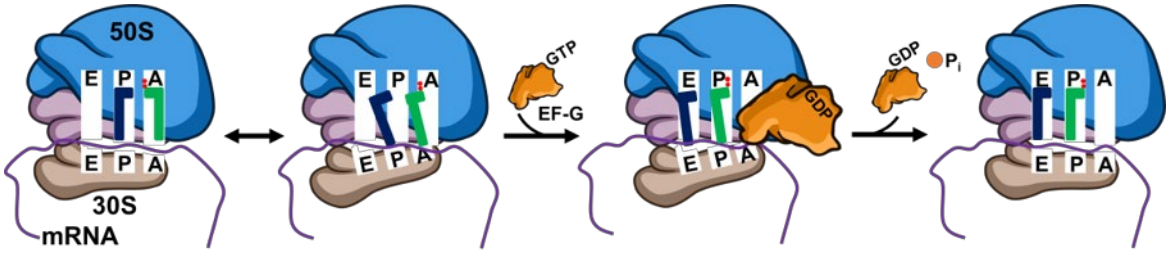

Figure 1. Schematic of ribosome translocation catalyzed by EF-G. Both the A-site and P-site undergo spontaneous conformational changes induced by the rotation of the 30S head region. EF-G binds near the A-site, catalyzing tRNA translocation and advancing the mRNA one-codon via the hydrolysis of one GTP molecule before dissociating from the ribosomal complex.

Quantifying EF-G power stroke has been a technical challenge. Three major experimental approaches have been reported in the literature.[12-14] We first reported the power stroke of 89 pN using a series of DNA-mRNA duplexes as force gauges. We also showed that this force is directional, which is consistent with the ribosome's moving direction and EF-G conformational changes.[12] Liu *et al.* used optical tweezers to pull the ribosome-mRNA system, in which the ribosome was immobilized on the surface and mRNA was labeled with a bead controlled by the optical tweezers. A smaller power stroke of 13 pN was concluded.[13] The results by Chen and co-workers using an indirect method favored the model with significant power stroke; however, no specific value was derived.[14] We later demonstrated that the power stroke was reduced when EF-G was crosslinked to restrict its conformational change; power stroke could also be reduced by the binding of fusidic acid that constrains EF-G conformational changes.[15] However, no correlation between power stroke and translocation fidelity has been observed, possibly because no alteration

was attempted for the critical domain IV of EF-G. In addition, none of the previous force measurements have directly compared the power stroke to a well-defined mechanical force acting on the same ribosome complex. A more refined experimental approach is needed to enhance the quantification of force amplitude.

On the technical front, various force spectroscopies have been developed, including atomic force spectroscopy, optical tweezers, magnetic tweezers, and acoustic force spectroscopy.[16-20] Broad biophysical applications have been reported, although rarely have there been examples on the complicated ribosome system. Based on quantum sensing, we invented super-resolution force spectroscopy (SURFS) by integrating acoustic force with atomic magnetometry.[21] DNA probes labeled with magnetic beads form duplexes with the mRNA of the ribosome complex. Precise external forces were applied to dissociate the duplexes, which was measured as a decrease in the magnetic signal by an atomic magnetometer, arguably the most sensitive device for magnetic detection.[22-25] We have achieved 0.4 pN force resolution, compared to the typical 10-20 pN force distribution by other force techniques. The step size of ribosome translocation can be monitored with sub-nucleotide precision.[26]

In this work, we report a unique combination of methods that measure power stroke with internal calibration and determine translocation steps from both ends of the ribosome, in the presence of mutated EF-Gs at two critical residues. Power stroke and acoustic force were applied sequentially onto the same ribosome systems, which yields precise percentages of DNA-mRNA force gauges dissociated by each force. The translocation steps were determined with single-nt resolution for both sides of the ribosome. We show direct evidence that a weaker power stroke by one mutated EF-G induced "-1" frameshift, whereas the other mutated EF-G generated the same power stroke as the wild type and did not induce frameshifting. The clear correlation between

power stroke and translocation fidelity shows the important role of specific noncovalent bonds between EF-G domain IV and tRNA in maintaining the correct reading frame in protein synthesis.

RESULTS

GTPase of EF-Gs

Two point mutations were performed on EF-G, Q508K and H584K, which were chosen due to their critical interactions with the A-site tRNA during translocation (Figure 2a).[27] Structurally, the glutamine-to-lysine mutation, which is not studied in the literature, removes the carbonyl structure from the residue and increases the length by one carbon. Both residues are polar, which may allow the mutation to maintain its hydrogen bonding with A37 of the A-site tRNA. In contrast, the histidine-to-lysine mutation causes a significantly structural change, eliminating the heterocyclic imidazole ring, which may disrupt its specific interaction with residue 36 of the tRNA, the leading position of codon-anticodon helix during translocation.[11, 28] The mutations were introduced using polymerase chain reaction (PCR) and purified using fast protein liquid chromatography (FPLC) (Supplementary Information, Scheme S1). Purified mutations were quantified using sodium dodecyl sulfate-polyacrylamide gel electrophoresis (SDS-PAGE) (Figure 2b, Supplementary Information, Figure S1), and sequencing confirmed the correct mutations (Supplementary Information, Figure S2).

GTPase assays were performed on mutated and nonmutated EF-G to determine the mutagenesis effects on protein activity. The unmutated EF-G, named as M5 in this work, served as the template for introducing mutations and has been shown to support normal translocation.[29] Thin layer chromatography (TLC) assay was used to determine the kinetics and overall percentages of fluorescently active mant-GTP hydrolyzed to mant-GDP (Figure 2c). The rates

were 0.19±0.03 min^{-1}, 0.19±0.03 min^{-1}, and 0.12±0.04 min^{-1} for H584K, Q508K, and M5, respectively. These results indicate that both mutated EF-Gs exhibited hydrolysis rates compared to M5, consistent with previous reports.[11] In addition, total GTP hydrolysis was higher in both mutants (97% for H584K and 96% for Q508K) compared to M5 (58%). However, this discrepancy is within 2-fold range; its significance remains unclear, as the GTPase center is far from the mutation sites. Meanwhile, dissociation constants for GTP and GDP binding (Supplementary Information, Figure S3) were determined using an established method from the literature.[30] The values, plotted in Figures 2d and 2e, are within reasonable experimental variations compared to prior reports.[30-33]

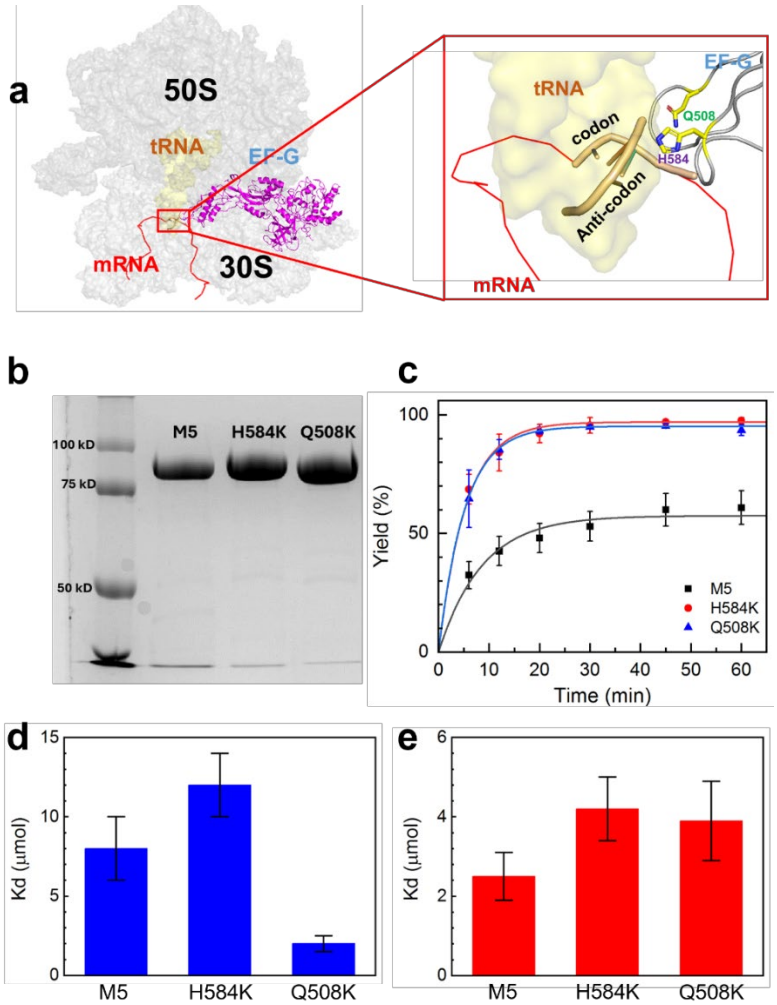

Figure 2. EF-G domain IV mutations and GTPase activity. **a)** Ribbon structure of ribosome, tRNA and EF-G (PDB: 4w29). The closeup view highlights H-bonding between tRNA and residues H584 or Q508, depicted in the red box. **b)** 8% SDS-PAGE gel of EF-G mutants following FPLC purification. **c)** Mant-GTP hydrolysis as determined by time-mediated TLC. Data were fitted with a pseudo first-order reaction equation. **d)** Mant-GTP binding and **e)** Mant-GDP binding. K_d was calculated via a mant-GTP and mant-GDP titration procedure published previously.

Power stroke of EF-Gs

Power stroke measurements are shown in Figure 3. A series of DNA probes, DNA_12 to DNA_19, were used to form 12-19 bp duplexes, respectively, with the 3′ end of the mRNA. Subsequently these duplexes were used as force rulers to gauge the EF-G power stroke. When the power stroke was greater than the dissociation force of the DNA-mRNA duplexes, a percentage of the duplexes would dissociate, indicated as a decrease in the magnetic signal.[15] This is because of the randomization of the magnetic dipoles of the dissociated beads attached to the 5' end of mRNA. To accurately determine the dissociation percentage, we applied acoustic force to dissociate all the remaining duplexes after EF-G's power stroke (Figure 3a). Therefore, the dissociation due to power stroke can be calculated from dividing the magnetic signal decrease due to power stroke by the overall signal decrease after applying sonication. This new approach provides direct signal calibration compared to our previous work in which the percentages were normalized to the shortest force ruler, although the same power stroke results were obtained. The magnetic signal of the samples was measured by translating the sample to a downstream atomic magnetometer at ~200 mm from the location of force application (Supplementary Information, Scheme S2). The sensitivity was approximately 300 $fT/Hz^{1/2}$.[34]

Figure 3b shows three typical magnetic signal changes for rulers at three different lengths and under two different forces. In the top panel for 12 bp duplexes, a large decrease of 59 pT was observed by EF-G power stroke and no additional decrease was observed for acoustic force. For 15 bp duplexes (middle panel), the signal decrease due to EF-G is 30 pT, indicating that EF-G power stroke exceeds the dissociation force of the duplex; further applying acoustic radiation force produced another signal decrease, at approximately 30 pT. This means the overall yield of the duplex was 60 pT, out of which 50% were dissociated by EF-G power stroke. The last case is for 18 bp duplexes, in which no dissociation was observed by EF-G (bottom panel). Therefore, the dissociation percentage is zero and there is no need for applying acoustic force.

Using this method, we plotted the dissociation percentages for 12-19 bp duplexes in the presence of three different EF-Gs (Figure 3c). For both M5 and Q508K, the onset of dissociation occurred at 17 bp, which are consistent with our previous works.[12, 15] Therefore, the power stroke for both EF-Gs was 89±11 pN. For H584K, however, the onset was at approximately 15 bp (14.8 bp for the intercept for the red plot on Figure 3c). Given the dissociation force for 14 and 15 bp being 50.1 and 62.0 pN, respectively[34] (Supplementary Information, Figure S4), H584K's power stroke was determined to be only 60±6 pN. This amplitude is similar to that of EF-G crosslinked by a short molecular linker or EF-G bound with fusidic acid.[15]

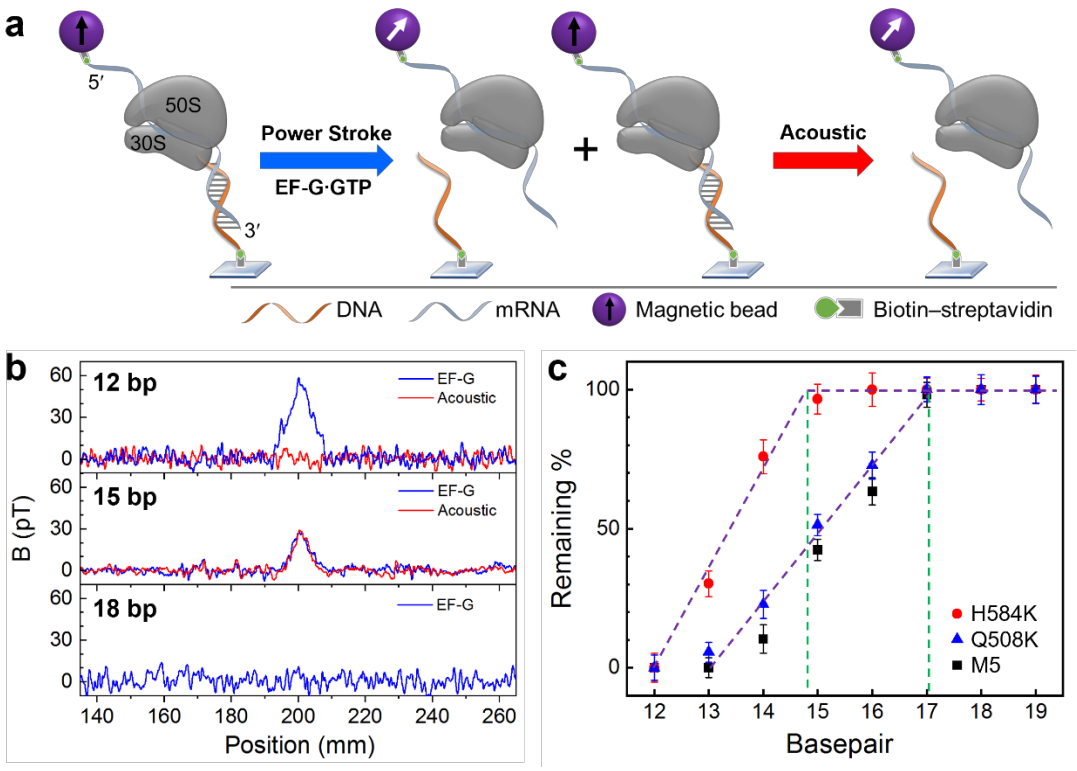

Figure 3. Power stroke of EF-Gs. **a)** Measuring method. The ribosome complex forms mRNA-DNA duplex at the 3′ end and is labeled with a magnetic bead at the 5′ end. EF-G power stroke will first induce duplex dissociation, and then the remaining duplex will then be dissociated by acoustic force. **b)** Magnetic signal changes for three different bps under EF-G power stroke and acoustic force. **c)** Plots of remaining duplexes for duplexes of 12-19 bps, in the presence of EF-Gs. The green lines indicate the onset of the dissociated duplex by EF-Gs.

Ribosome translocation and frameshifting

To reveal potential differences in translocation fidelity for the mutated EF-Gs, we used the SURFS technique to probe the translocation steps from both 5′ and 3′ ends of the mRNA with single-nt resolution, which has been well established in our groups. Figure 4a illustrates the detection scheme. The ribosome pre-translocation complex (Pre) was immobilized on the surface

via the biotin on the 5′ end of the mRNA. A DNA probe was then incubated with the Pre complex to form duplexes with the exposed mRNA, at either the 5′ or 3′ end. For the 5′ end, the DNA probe forms 12 bp duplexes with dissociation force of 21 pN, and would form 15-bp duplex with the Post complex if the ribosome undergoes normal translocation with dissociation force of 52 pN. If the ribosome translocates only two nucleotides, 14 bp duplexes will be formed, which will be indicated by a weaker force of 45 pN. With force resolution of ~2 pN in this work, we can easily distinguish the translocation steps of the ribosome. Similarly for the 3′ end, 14 bp duplexes will be formed between the DNA probe and Pre, and 11 bp for Post for normal translocation but 12 bp for "-1" frameshifting (Supplementary Information, Figure S3). Results in Figure 4b showed that the ribosome underwent normal translocation in the presence of Q508K or M5, in which it translocated by 3 nts from both the 5′ and 3′ ends of the mRNA. This correlates well with the normal power stroke of Q508K compared to M5. However, for H584K, which was only able to produce a much reduced power stroke, the ribosome translocated by 2 nts, i.e., "-1" frameshifting occurred. This result is consistent with previous studies on H584 mutation.[10, 11] It is also interesting that the ribosome has the same displacements at the 5′ and 3′ ends. In other words, the mRNA threaded through the ribosome smoothly; no looped intermediate state was formed. These observations strongly suggest that EF-G power stroke is important for the ribosome to maintain the reading frame during translocation.

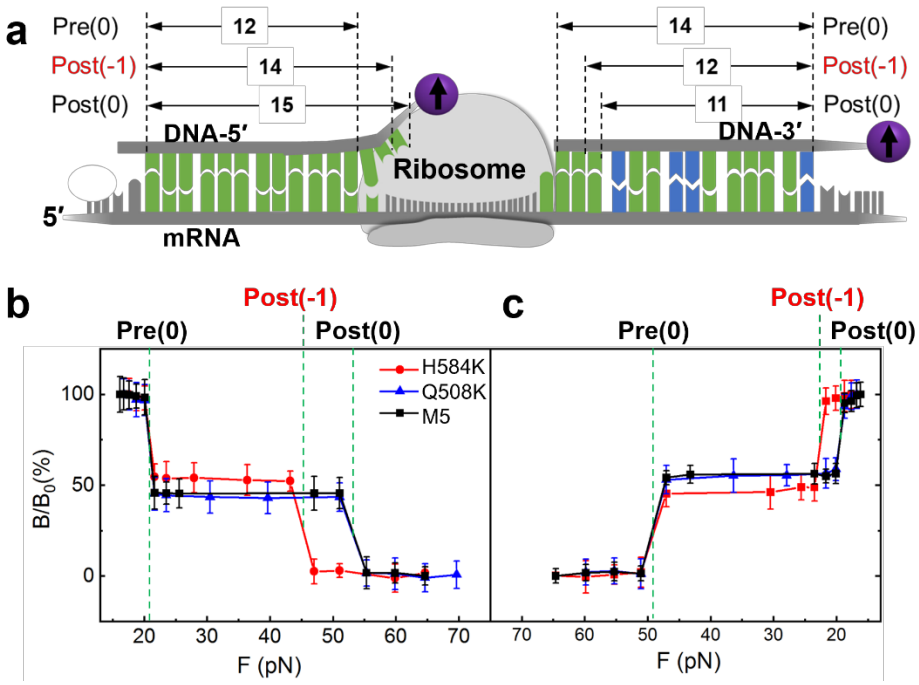

Figure 4. Translocation by EF-Gs. **a)** Probing scheme. The ribosome pre-translocation complex (Pre) was immobilized on the surface. DNA-5′ and DNA-3′ were used to probe ribosome motion on the 5′- and 3′-end of the mRNA, respectively. Pre(0) and Post(0) are the normal reading frame; Post(-1) is for "-1" frameshift in which the ribosome moved by 2 nts. The numbers with arrows indicate duplex bps between DNA probes and the exposed mRNA segments in the ribosome complex. **b)** Force spectra for the 5′ (left) and 3′ (right). The transitions were assigned to different ribosome states based on the force values.

DISCUSSION

The clear correlation between a weaker power stroke and a reduced translocation step provides the first mechanical evidence demonstrating the vital role of specific interactions between EF-G and tRNA. A strong coupling allows EF-G to drive the full 3-nt translocation, while alteration of these interactions causes EF-G to be less effective. Consequently, translation errors such as "-1" frameshifting may occur (Figure 5). Structural studies have shown that EF-G interacts with A-site

tRNA via H584 and Q508 residues by noncovalently bonding with tRNA's U36 and A37 nucleotides, respectively.[10, 11, 28] The H584K mutation likely altered the orientation of its interaction with the leading base pair of the minihelix along the translocation direction (Figure 5). Consequently, changes in force projection on the mRNA moving trajectory and the pivotal point on tRNA would reduce the power stroke's effect on the activation energy barrier, according to the Bell's model.[12] Applying the same Bell's model, the deceleration factor is approximately 40-folds for the 30 pN force decrease we observed at 25 °C, which is close to the 100-fold deceleration effect reported earlier.[35] If changes in the pivotal point further increase the transition state distance, this effect could be even greater. In contrast, Q508K mutation was less likely to generate much structural changes. Therefore, we propose that the power stroke likely plays multifaceted roles in regulating translocation, influencing not only through its amplitude but also via atomic-level interactions with the ribosome complex. The previously observed decrease in kinetics for H584K was attributed to increased frameshifting yield.[10, 11] Our results here imply that this effect is likely due to altered force projection and a shifted pivotal point, leading to a less-reduced activation barrier and consequently slower translocation.

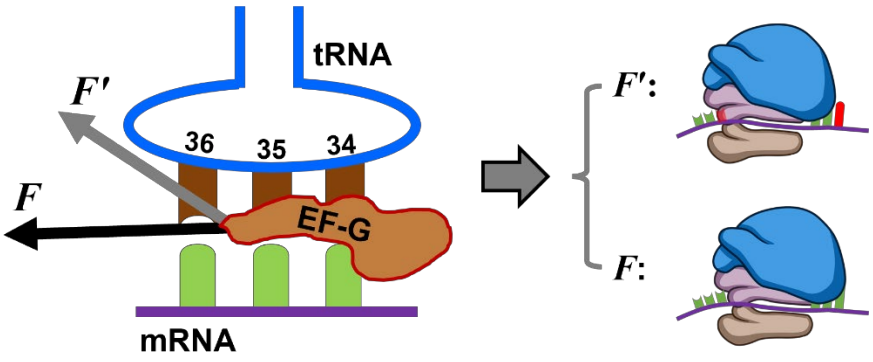

Figure 5. Altering EF-G–tRNA bonding causes translation error. The black arrow represents the normal specific EF-G–tRNA bonding that produces high power stroke *F*. It leads to the correct reading frame after translocation, in which the ribosome translocates 3 nt on mRNA

from both sides (right, bottom case). The grey arrow indicates the weakened interaction for mutated EF-G H584K, producing weakened power stroke F'. It correlates with "-1" frameshift in which the ribosome moved only 2 nts for both sides of the mRNA (right, top case).

Our methods of using nucleic acids to probe power stroke and ribosome displacement offer a unique perspective for investigating complex biomolecular functions. The combination of DNA force gauges and external force provides a viable approach to precisely determine the mechanical forces involved in protein conformational changes, which are difficult to be directly measured by optical- or fluorescence-based techniques. The application of quantum sensing with DNA rulers provides sub-nt resolution for molecular motion gives precise location displacement information that complements structural techniques and force measurements. This work shows that broader applications in chemical and biological research can be expected for innovative nucleic acid-based techniques.

METHODS

EF-G mutation and characterization

Site-directed mutagenesis of *Escherichia coli* was performed using a Q5® High-Fidelity DNA Polymerase kit (New England Biolabs, NEB) via polymerase chain reaction (PCR). Forward and reverse primers were designed using NEB Base Changer and purchased through Integrated DNA Technologies (IDT). The completed PCR reaction product was transformed into MAX Efficiency® DH5α™-T1R competent cells (ThermoFisher Scientific) and grown on Lysogeny Broth-Kanamycin (LB-Kan) agar plates overnight at 37°C. pDNA from colonies was isolated using an PureLink™ HQ Mini Plasmid DNA Purification Kit (ThermoFisher Scientific) and sequenced via

Sanger sequencing. Sequenced mutants were transformed into One Shot™ BL21(DE3) cells (ThermoFisher Scientific) and grown in 3 liters of LB-Kan liquid medium until cultures entered log phase. The cultures were then induced using 1 M isopropyl ß-D-1-thiogalactopyranoside (IPTG) and incubated for three hours at 37ºC while shaking. Cells were lysed using lysozyme, DNase I, and bacterial extraction reagent (0.7% (w/v) n-octyl-1-thio-beta-D-glucopyranoside, 0.2% (w/v) Nonidet P-40, 0.1% (w/v) Triton™ X-100, 50 mM Tris-Acetate (pH 7.60), 1 mM $MgCl_2$, 0.5 mM $CaCl_2$, and 0.1 mM EDTA Sodium Salt (pH 8.00)). Cell debris was pelleted, and the cell lysate was cycled through a 5 mL HisTrap™ HP His tag protein purification column (Cytiva Life Sciences) using a Pharmacia LKB P-1 pump for three hours. The cycled Ni^{2+} column was connected to a ÄKTApurifier Fast Protein Liquid Chromatograph (FPLC) system, and the column was flushed with protein lysis buffer (50 mM NaH_2PO_4, 150 mM NaCl, and 4 mM BME, all from Sigma-Aldrich, pH 8.0). Protein was eluted using a gradient of protein elution buffer (50 mM NaH_2PO_4, 150 mM NaCl, 4 mM BME, 1 M imidazole (Sigma-Aldrich), pH 8.0). FPLC fractions were quantified via SDS-PAGE and fractions containing purified EF-G were stored in protein storage buffer (20 mM Tris-HCl, 10 mM $MgCl_2$, 40 mM KCl, 4 mM BME, pH=7.5) at -80ºC.

Preparation of the ribosome complex

The 70S ribosomes were purified from *E. coli* MRE600 as previously described. A culture of *E. coli* MRE600 was propagated in LB medium in a shaker incubator at 37°C and 200 rpm (revolution per minute) until optical density at 600 nm reached value of 0.6. The cells were harvested by centrifugation at 3,000×*g*, 4 °C, for 20 minutes. The cell pellet was washed with cold buffer I (50 mM Tris-HCl, pH 7.6, 10 mM $MgCl_2$, 100 mM NH_4Cl, 6 mM BME, 0.5 mM EDTA).

Then the cells were resuspended in the same buffer with 0.2 mg/mL egg white lysozyme and 2 μg/mL DNase I and incubated for 30 min on ice. Afterward the cells were lysed by sonication for 5 minutes (10 s pulse, 20 s pause) on ice. Cell debris were removed by two consecutive centrifugations at 14,500×*g*, 4 °C, for 1 hour each. Cleared supernatant was layered on top of pre-cooled 1.1 M sucrose cushion in buffer II (20 mM Tris-HCl, pH 7.6, 10 mM $MgCl_2$, 500 mM NH_4Cl, 6 mM BME, 0.5 mM EDTA) with volume ratio 1:1, respectively. The ribosomes were pelleted by centrifugation on Beckman XL-80 ultracentrifuge with Type 45 Ti Fixed-Angle rotor at 120,000×*g*, 4 °C, for 20 hours. The collected pellet was carefully rinsed with buffer I, then the ribosomes were resuspended in the same buffer, and the concentration of NH_4Cl was adjusted to 400 mM. The ribosomes were pelleted again by ultracentrifugation at 120,000×*g*, 4 °C, for 20 hours. The pellet was rinsed with buffer I and finally resuspended in minimum volume of the same buffer. The ribosome concentration was determined by UV absorbance measurement at 260 nm using conversion coefficient 1 A260 unit = 23 pmol (10^{-12} mol) of 70S ribosomes. The prepared ribosome solution was aliquoted, flash-frozen in liquid nitrogen, and stored at -80 °C.

All the mixtures were in TAM_{10} buffer, which consisted of 20 mM Tris-HCl (pH 7.5), 10 mM $MgCl_2$, 30 mM NH_4Cl, 70 mM KCl, 0.5 mM EDTA, and 7 mM BME (2-mercaptoethanol). Three mixtures were prepared: the ribosome mix, Tu0G mix, Phe mix. The ribosome mix contains 1 μM ribosome, 1.5 μM each of initiation factors IF1, IF2, IF3, 2 μM of mRNA, 4 μM of charged fMet-$tRNA^{fMet}$, and 4 mM of GTP. The Tu0G mix contained 4 μM EF-Tu, 4 mM GTP, 4 mM 2-phosphoenolpyruvate (PEP), and 0.02 mg/mL Pyruvate Kinase. The Phe mix contained 100 mM Tris (pH 7.8), 20 mM $MgCl_2$, 1 mM EDTA, 4 mM ATP, 7 mM BME, 2 μM $tRNA^{Phe}$ synthetase (PheRS), 2 A_{260} units/mL $tRNA^{Phe}$, and 0.25 mM phenylalanine. The ribosome mix, Tu0G mix, and Phe mix were combined in a volume ratio of 1:2:2, then incubated at room temperature for 2

minutes. The resulting MF-Pre ribosome complex was added on top of 1.1 M sucrose cushion and purified by centrifugation with a Hitachi CS150FNX ultracentrifuge (S140AT rotor, 200,000-400,000×*g*, 4 °C, 3 hours).

Power stroke measurement

The sample wells were of 4×3 mm^2 area formed by glueing a piece of biotin-coated glass with a plastic holder (2 mm thick). After incubating with 0.25 mg/mL streptavidin for 50 minutes, the extra streptavidin was rinsed twice with water. The probing DNA strand was immobilized on the surface and incubated for 1 hour. After rinsing once with TAM10 buffer, the MF-Pre ribosome complex was added and incubated overnight to form duplexes with DNA. Afterward, the magnetic beads were added into the sample well and incubated for 2 hours. The sample was magnetized for 2 minutes using a permanent magnet (~0.5 T) and centrifuged (5427R, Eppendorf) at 820×*g* for 20 minutes to remove non-specifically bound magnetic particles. The initial magnetic signal of the samples was measured by a home-built atomic magnetometer. The EF-G was added and incubated with duplexes for 1hr. The magnetic signal of the samples was measured again before and after applied acoustic force. The total magnetic signal was obtained by the magnetic signal before EF-G subtracting the signal after the acoustic force. The remnant magnetic signal was obtained by the magnetic signal after EF-G subtracting the signal after the acoustic force. Percentages of remnant magnetic beads were obtained by dividing the remnant magnetic signal by the total magnetic signal.

The mRNA sequence is 5′-Bio/ C AAC UGU UAA UUA AAU UAA AUU AAA AAG GAA AUA AAA AUG UUU GAA AA<u>A</u> <u>AAG</u> <u>UAC</u> <u>GUA</u> <u>AAU</u> <u>CUA</u> <u>CUG</u> CUG AAC UC-3′. The

underscored nucleotides will form 12-19 bp duplexes with the DNA force rulers depending on the lengths of the respective rulers. The DNA rulers are:

PSNew_12: 5′-/BioTEG/CT CAA GTC GTC ATC TTT TAC GTA CTT T-3′

PSNew_13: 5′-/BioTEG/CT CAA GTC GTC ATC ATT TAC GTA CTT T-3′

PSNew_14: 5′-/BioTEG/CT CAA GTC GTC ATG ATT TAC GTA CTT T-3′

PSNew_15: 5′-/BioTEG/CT CAA GTC GTC AAG ATT TAC GTA CTT T-3′

PSNew_16: 5′-/BioTEG/CT CAA GTC GTC TAG ATT TAC GTA CTT T-3′

PSNew_17: 5′-/BioTEG/CT CAA GTC GTG TAG ATT TAC GTA CTT T-3′

PSNew_18: 5′-/BioTEG/CT CAA GTC GAG TAG ATT TAC GTA CTT T-3′

PSNew_19: 5′-/BioTEG/CT CAA GTC CAG TAG ATT TAC GTA CTT T-3′

The underscored nucleotides are complementary to the mRNA sequence.

Ribosome translocation and frameshifting

The sample wells were the same as in the power stroke experiments. The difference is that the MF-Pre ribosome complex was immobilized on the surface via the 5′-end biotin on the mRNA by incubating for 1 hour. In the case of post complex, 1 μM Pre complex was incubated with 2 μM EF-G, 4 mM GTP, 4 mM PEP, and 0.02 mg/mL pyruvate kinase at 37 ºC for 30 minutes. Then, 1 μM probing DNA was added and incubated overnight to form duplexes with the uncovered mRNA in the ribosome complex. Afterward, streptavidin-coated magnetic beads (M280) were introduced into the sample well and incubated for 2 hours. Before the force measurements, the sample was magnetized for 2 minutes using a permanent magnet (~0.5 T) and centrifuged (5427R, Eppendorf) at 820×*g* for 20 minutes to remove non-specifically bound magnetic particles.

The sequence for the 3′ DNA probe is 5′-/BioTEG/CTC AAG TCG TCA T*GA TTT ACG TAC TTT*-3′, which forms 14 bp duplex with pre-translocation ribosome complex. The sequence for the 5′ DNA probe is 5′-/BioTEG/T_{50} AAA TTA *ATT TAA TTT AAT*-3′, which forms 12 bp duplex with the pre-translocation ribosome complex.

Acknowledgements

This work was supported by the US National Institutes of Health (R01GM111452, Y.W., S.X.) and National Science Foundation (2130427, S.X., Y.W.). J.H.S. was supported by US National Institutes of Health (3R01GM111452-07S1).

Author contributions

Y.W. and S.X. designed the overall project. J.H.S. and Y.W. prepared the samples and performed the biological assays. Y.C. performed force measurements and translocation. All authors contributed to data analysis, discussion, and preparation of the manuscript.

Competing interests

The authors declare no competing interests.

Additional information

Supplementary material is available online.

Data Availability

The datasets generated and/or analyzed during the current study are available in the UniProt repository, SPIN200033120 and SPIN200033125.

References

1. Noller HF. The ribosome comes to life. Cell. 2024;187(23):6486-500. doi: 10.1016/j.cell.2024.10.035. PubMed PMID: 39547209.
2. Agirrezabala X, Frank J. Elongation in translation as a dynamic interaction among the ribosome, tRNA, and elongation factors EF-G and EF-Tu. Q Rev Biophys. 2009;42(3):159-200. doi: 10.1017/S0033583509990060. PubMed PMID: 20025795; PMCID: PMC2832932.
3. Bose T, Fridkin G, Davidovich C, Krupkin M, Dinger N, Falkovich AH, Peleg Y, Agmon I, Bashan A, Yonath A. Origin of life: protoribosome forms peptide bonds and links RNA and protein dominated worlds. Nucleic Acids Res. 2022;50(4):1815-28. doi: 10.1093/nar/gkac052. PubMed PMID: 35137169; PMCID: PMC8886871.
4. Yamamoto H, Qin Y, Achenbach J, Li C, Kijek J, Spahn CM, Nierhaus KH. EF-G and EF4: translocation and back-translocation on the bacterial ribosome. Nat Rev Microbiol. 2014;12(2):89-100. Epub 20131223. doi: 10.1038/nrmicro3176. PubMed PMID: 24362468.
5. Choi J, Grosely R, Prabhakar A, Lapointe CP, Wang J, Puglisi JD. How Messenger RNA and Nascent Chain Sequences Regulate Translation Elongation. Annu Rev Biochem. 2018;87:421-49. doi: 10.1146/annurev-biochem-060815-014818. PubMed PMID: 29925264; PMCID: PMC6594189.
6. Cornish PV, Ermolenko DN, Noller HF, Ha T. Spontaneous intersubunit rotation in single ribosomes. Mol Cell. 2008;30(5):578-88. doi: 10.1016/j.molcel.2008.05.004. PubMed PMID: 18538656; PMCID: PMC2491453.
7. Carbone CE, Loveland AB, Gamper HB, Jr., Hou YM, Demo G, Korostelev AA. Time-resolved cryo-EM visualizes ribosomal translocation with EF-G and GTP. Nat Commun. 2021;12(1):7236. Epub 20211213. doi: 10.1038/s41467-021-27415-0. PubMed PMID: 34903725; PMCID: PMC8668904.
8. Petrychenko V, Peng BZ, de APSAC, Peske F, Rodnina MV, Fischer N. Structural mechanism of GTPase-powered ribosome-tRNA movement. Nat Commun. 2021;12(1):5933. Epub 20211011. doi: 10.1038/s41467-021-26133-x. PubMed PMID: 34635670; PMCID: PMC8505512.
9. Poulis P, Peske F, Rodnina MV. The many faces of ribosome translocation along the mRNA: reading frame maintenance, ribosome frameshifting and translational bypassing. Biol Chem. 2023;404(8-9):755-67. Epub 20230421. doi: 10.1515/hsz-2023-0142. PubMed PMID: 37077160.
10. Niblett D, Nelson C, Leung CS, Rexroad G, Cozy J, Zhou J, Lancaster L, Noller HF. Mutations in domain IV of elongation factor EF-G confer -1 frameshifting. RNA. 2021;27(1):40-53. Epub 20201002. doi: 10.1261/rna.077339.120. PubMed PMID: 33008838; PMCID: PMC7749637.
11. Peng BZ, Bock LV, Belardinelli R, Peske F, Grubmuller H, Rodnina MV. Active role of elongation factor G in maintaining the mRNA reading frame during translation. Sci Adv. 2019;5(12):eaax8030. Epub 20191220. doi: 10.1126/sciadv.aax8030. PubMed PMID: 31903418; PMCID: PMC6924986.
12. Yao L, Li Y, Tsai TW, Xu S, Wang Y. Noninvasive measurement of the mechanical force generated by motor protein EF-G during ribosome translocation. Angew Chem Int Ed Engl. 2013;52(52):14041-4. Epub 20131107. doi: 10.1002/anie.201307419. PubMed PMID: 24353228.
13. Liu T, Kaplan A, Alexander L, Yan S, Wen JD, Lancaster L, Wickersham CE, Fredrick K, Noller H, Tinoco I, Bustamante CJ. Direct measurement of the mechanical work during translocation by

the ribosome. Elife. 2014;3:e03406. Epub 20140811. doi: 10.7554/eLife.03406. PubMed PMID: 25114092; PMCID: PMC4126342.
14. Chen C, Cui X, Beausang JF, Zhang H, Farrell I, Cooperman BS, Goldman YE. Elongation factor G initiates translocation through a power stroke. Proc Natl Acad Sci U S A. 2016;113(27):7515-20. Epub 20160616. doi: 10.1073/pnas.1602668113. PubMed PMID: 27313204; PMCID: PMC4941437.
15. Yin H, Gavriliuc M, Lin R, Xu SJ, Wang YH. Modulation and Visualization of EF-G Power Stroke During Ribosomal Translocation. Chembiochem. 2019;20(23):2927-35. doi: 10.1002/cbic.201900276. PubMed PMID: WOS:000500160700006.
16. Rief M, Clausen-Schaumann H, Gaub HE. Sequence-dependent mechanics of single DNA molecules. Nat Struct Biol. 1999;6(4):346-9. doi: 10.1038/7582. PubMed PMID: 10201403.
17. Bustamante C, Bryant Z, Smith SB. Ten years of tension: single-molecule DNA mechanics. Nature. 2003;421(6921):423-7. doi: 10.1038/nature01405. PubMed PMID: 12540915.
18. Yangyuoru PM, Dhakal S, Yu Z, Koirala D, Mwongela SM, Mao H. Single-molecule measurements of the binding between small molecules and DNA aptamers. Anal Chem. 2012;84(12):5298-303. Epub 20120601. doi: 10.1021/ac300427d. PubMed PMID: 22702719.
19. Liu C, Kubo K, Wang E, Han KS, Yang F, Chen G, Escobedo FA, Coates GW, Chen P. Single polymer growth dynamics. Science. 2017;358(6361):352-5. doi: 10.1126/science.aan6837. PubMed PMID: 29051377.
20. Sitters G, Kamsma D, Thalhammer G, Ritsch-Marte M, Peterman EJG, Wuite GJL. Acoustic force spectroscopy. Nat Methods. 2015;12(1):47-50. doi: DOI 10.1038/nmeth.3183. PubMed PMID: WOS:000347668600016.
21. Jia HN, Wang YH, Xu SJ. Super-resolution force spectroscopy reveals ribosomal motion at sub-nucleotide steps. Chem Commun. 2018;54(46):5883-6. doi: 10.1039/c8cc02658k. PubMed PMID: WOS:000434385600018.
22. Budker D, Kimball DF, Rochester SM, Yashchuk VV. Nonlinear magneto-optical rotation via alignment-to-orientation conversion. Phys Rev Lett. 2000;85(10):2088-91. doi: 10.1103/PhysRevLett.85.2088. PubMed PMID: 10970469.
23. Kominis IK, Kornack TW, Allred JC, Romalis MV. A subfemtotesla multichannel atomic magnetometer. Nature. 2003;422(6932):596-9. doi: 10.1038/nature01484. PubMed PMID: 12686995.
24. Shah V, Knappe S, Schwindt PDD, Kitching J. Subpicotesla atomic magnetometry with a microfabricated vapour cell. Nature Photonics. 2007;1(11):649-52. doi: 10.1038/nphoton.2007.201.
25. Boto E, Shah V, Hill RM, Rhodes N, Osborne J, Doyle C, Holmes N, Rea M, Leggett J, Bowtell R, Brookes MJ. Triaxial detection of the neuromagnetic field using optically-pumped magnetometry: feasibility and application in children. Neuroimage. 2022;252. doi: ARTN 119027 10.1016/j.neuroimage.2022.119027. PubMed PMID: WOS:000819915900004.
26. Mao Y, Lin R, Xu S, Wang Y. High-Resolution DNA Dual-Rulers Reveal a New Intermediate State in Ribosomal Frameshifting. Chembiochem. 2021;22(10):1775-8. Epub 20210225. doi: 10.1002/cbic.202000863. PubMed PMID: 33458897; PMCID: PMC8014572.
27. Li W, Liu Z, Koripella RK, Langlois R, Sanyal S, Frank J. Activation of GTP hydrolysis in mRNA-tRNA translocation by elongation factor G. Science Advances. 2015;1(4). doi: ARTN e1500169 10.1126/sciadv.1500169. PubMed PMID: WOS:000216593600012.
28. Hoffer ED, Hong S, Sunita S, Maehigashi T, Gonzalez RLJ, Whitford PC, Dunham CM. Structural insights into mRNA reading frame regulation by tRNA modification and slippery codon-anticodon pairing. Elife. 2020;9. Epub 20201005. doi: 10.7554/eLife.51898. PubMed PMID: 33016876; PMCID: PMC7577736.

29. Yin H, Gavriliuc M, Lin R, Xu S, Wang Y. Modulation and Visualization of EF-G Power Stroke During Ribosomal Translocation. Chembiochem. 2019;20(23):2927-35. Epub 20190920. doi: 10.1002/cbic.201900276. PubMed PMID: 31194278; PMCID: PMC6888950.
30. Wilden B, Savelsbergh A, Rodnina MV, Wintermeyer W. Role and timing of GTP binding and hydrolysis during EF-G-dependent tRNA translocation on the ribosome. P Natl Acad Sci USA. 2006;103(37):13670-5. doi: 10.1073/pnas.0606099103. PubMed PMID: WOS:000240648300023.
31. Mitkevich VA, Shyp V, Petrushanko IY, Soosaar A, Atkinson GC, Tenson T, Makarov AA, Hauryliuk V. GTPases IF2 and EF-G bind GDP and the SRL RNA in a mutually exclusive manner. Sci Rep-Uk. 2012;2. doi: ARTN 843
10.1038/srep00843. PubMed PMID: WOS:000311099600003.
32. Zavialov AV, Hauryliuk VV, Ehrenberg M. Guanine-nucleotide exchange on ribosome-bound elongation factor G initiates the translocation of tRNAs. J Biol. 2005;4(2):9. Epub 20050627. doi: 10.1186/jbiol24. PubMed PMID: 15985150; PMCID: PMC1175996.
33. Wriggers W, Agrawal RK, Drew DL, McCammon A, Frank J. Domain motions of EF-G bound to the 70S ribosome: insights from a hand-shaking between multi-resolution structures. Biophys J. 2000;79(3):1670-8. doi: 10.1016/S0006-3495(00)76416-2. PubMed PMID: 10969026; PMCID: PMC1301058.
34. Chen YJ, Gavriliuc M, Zeng Y, Xu SJ, Wang YH. Allosteric Effects of EF-G Domain I Mutations Inducing Ribosome Frameshifting Revealed by Multiplexed Force Spectroscopy. Chembiochem. 2024;25(19). doi: 10.1002/cbic.202400130. PubMed PMID: WOS:001293105100001.
35. Savelsbergh A, Matassova NB, Rodnina MV, Wintermeyer W. Role of domains 4 and 5 in elongation factor G functions on the ribosome. J Mol Biol. 2000;300(4):951-61. doi: 10.1006/jmbi.2000.3886. PubMed PMID: 10891280.

Supplementary Information

EF-G Mutations Reveal Correlation between Power Stroke and Translocation Fidelity in Protein Synthesis

Yanjun Chen,[1†] Jacob H. Steele,[2†] Shoujun Xu,[1*] Yuhong Wang[1,2*]

[1]Department of Chemistry, [2]Department of Biology and Biochemistry

University of Houston, Houston, TX 77204, USA

Table of Contents

1. Flowchart of the EF-G mutation, with *Scheme S1*;
2. SDS-PAGE gel photo of the mutated EF-Gs, with *Figure S1*;
3. Sequencing results of the mutated EF-Gs, with *Figure S2*;
4. GTP and GDP binding assay, with *Figure S3*;
5. Magnetic detection with optically pumped magnetometer, with *Scheme S2*;
6. Force calibration for the DNA-mRNA duplexes, with *Figure S4*.

1. Flowchart of EF-G mutation

The preparation procedure is summarized in the following scheme.

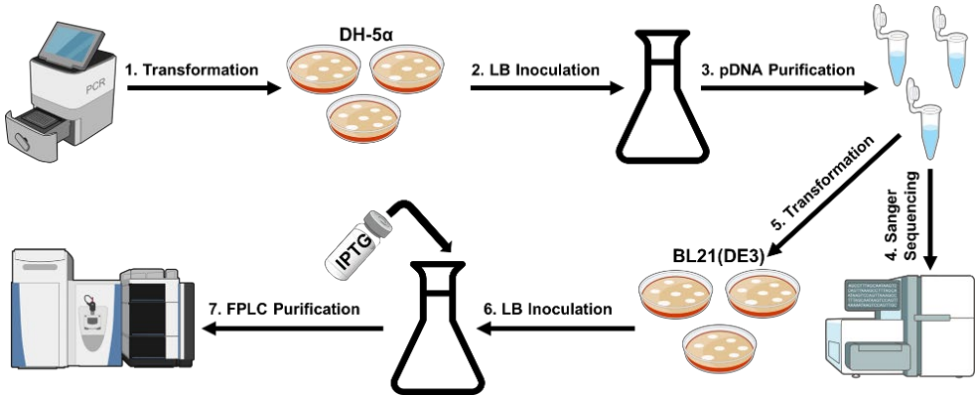

Scheme S1. EF-G mutagenesis flowchart.

2. SDS-PAGE gel photo of the mutated EF-Gs

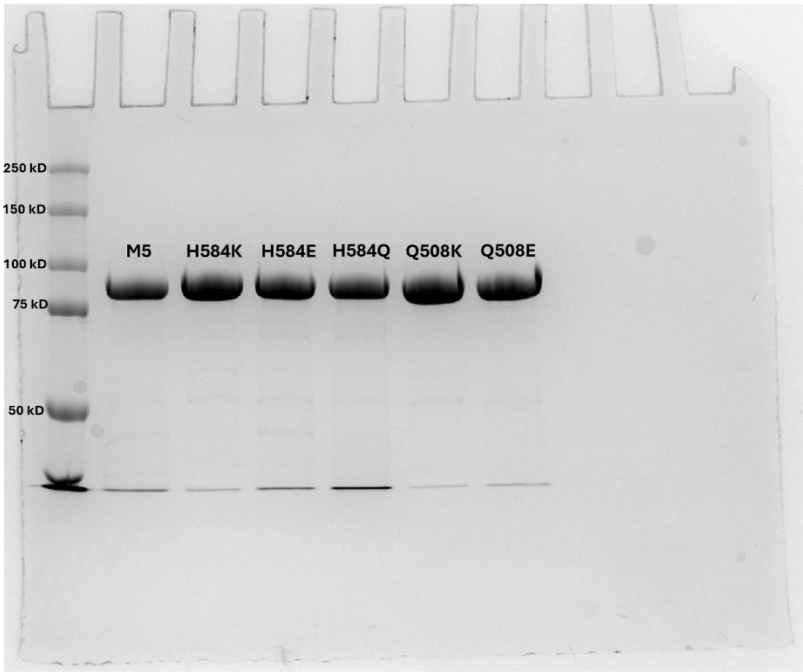

Figure S1. SDS-PAGE gel photo of five mutated EF-Gs. Two of the mutations, H584K and Q508K, are reported in this work.

3. Sequencing results of the mutated EF-Gs

The mutated EF-Gs were confirmed using Sanger sequencing (Figure S2) (Epoch Life Sciences). Sequencing was performed using T7 (5′–TAA TAC GAC TCA CTA TAG GG –3′), P2 (5′–GGT TCC GCT GCA GCT GG –3′), P3 (5′–CTC CGT GAA AGC TGC AC –3′), and P4 (5′–ACG AGT TCA TCA ACG AC –3′) primers. No offsite mutations or frameshifting was present due to non-selective forward and reverse primer binding during PCR.

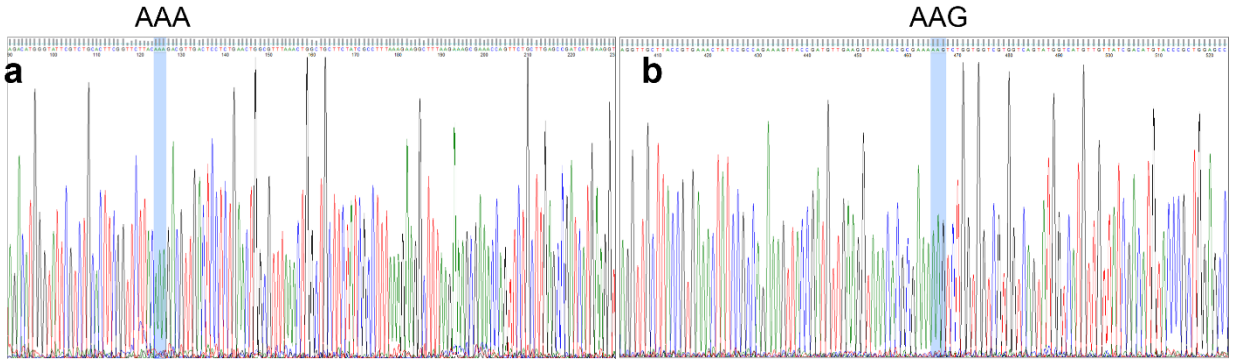

Figure S2. Sequencing results for **a**) H584K and **b**) Q508K. The new residue K is indicated by its genetic code AAA or AAG.

4. GTP and GDP binding assay

Mant-GXP (mant: 2′/3′-*O*-*N*-Methylanthraniloyl, X = T or D, both from Sigma Aldrich) binding assays were performed on EF-G M5 and domain IV mutant EF-G to determine the effects mutations have on GXP binding and dissociation. Both mant-GXP and EF-G solutions were prepared in TAM10 buffer with BME. The EF-G samples were then diluted with 40 μL of 36 μM Mant-GXP. The final concentrations of the samples were 32, 16, 8, 4, 2, and 0 μM following the addition of the mant-GXP solution. The final mant-GXP concentration was 16 μM following dilution. A blank sample was also made using only 50 μL of TAM10 buffer with BME. 40 μL of each concentration and blank was transferred to fluorescence tubes and the fluorescence

measurements were performed three times for each sample. The averaged values were fitted using the following equation to obtain binding affinity K:

$$y = 16A + \frac{B - A - D}{2}\left[(x + 16 + K) - \sqrt{|(x + 16 + K)^2 - 64x|}\right] + Dx + C$$

Here, A is mant fluorescence without EF-G, B is fluorescence of EF-G/mant-GXP to be fitted, C is offset for background, and D is fluorescence of EF-G only. For GTP, A = 2397.15, C= 133.76, D = 8.88; for GDP: A =1966.68, C = 130.84, D = 8.88.

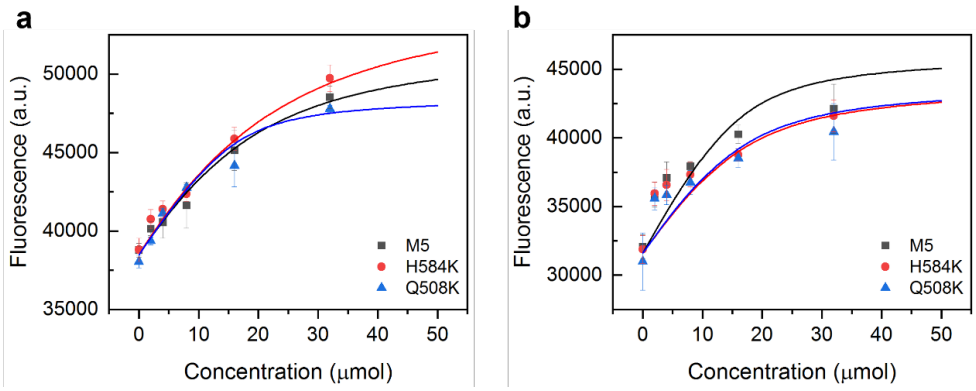

Figure S3. Determination of EF-G binding affinity with **a**) mant-GTP and **b**) mant-GDP.

5. Magnetic detection with optically pumped magnetometer

The following scheme shows the main components of the magnetic detection.

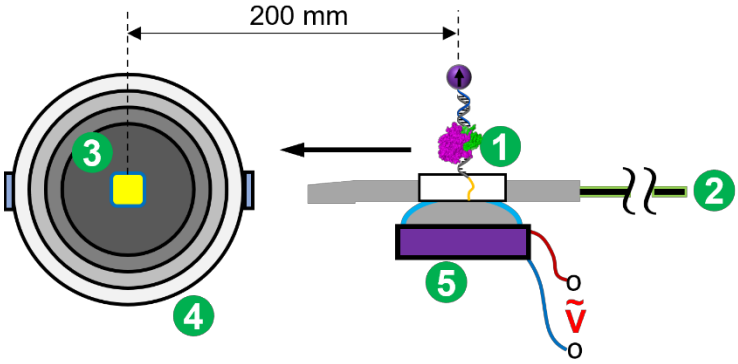

Scheme S2. Scanning magnetic detection with an optically pumped magnetometer. 1, sample with magnetically labeled ribosome system; 2, linear motor; 3, atomic sensor; 4, four-layer magnetic shield; 5, piezo to produce acoustic force.

6. Force calibration for the DNA-mRNA duplexes

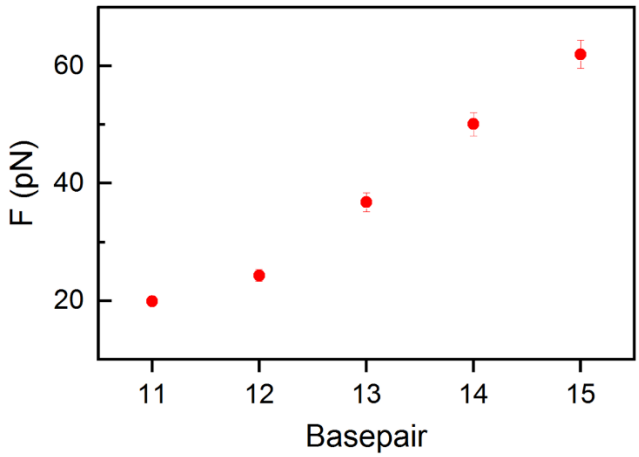

Figure S4. Force calibration for the DNA-mRNA duplexes.